Cell Host & Microbe, Volume *29*

Supplemental information

Aberrant gut-microbiota-immune-brain axis development in premature neonates with brain damage

David Seki, Margareta Mayer, Bela Hausmann, Petra Pjevac, Vito Giordano, Katharina Goeral, Lukas Unterasinger, Katrin Klebermaß-Schrehof, Kim De Paepe, Tom Van de Wiele, Andreas Spittler, Gregor Kasprian, Benedikt Warth, Angelika Berger, David Berry, and Lukas Wisgrill

Table S1. Likeliness of sample inclusion, Related to STAR Methods.

Sample type	Day 3	Day 7	Week 2	Week 4	Week 6	Week 8	Week 10	Week 12
Stool: 16S rRNA	0.77	0.72	0.87	0.74	0.77	0.81	0.66	0.4
Stool: SCFA	0.77	0.62	0.83	0.75	0.79	0.83	0.68	0.43
aEEG	0.68	0.72	0.75	0.64	0.66	0.62	0.47	0.3
NIRS	0.7	0.7	0.74	0.77	0.7	0.57	0.53	0.36

	Day 3	Day 7	Day 28	Corr. 32 weeks	Term age
T cell ontogeny	0.75	0.81	0.83	0.86	0.72
Cytokines/ Chemokines	0.75	0.83	0.81	0.78	0.67

Table S2. The 10 most abundant species of the premature infant gut microbiome, Related to Figure 1.

Sequence ID	Genus	16S rRNA gene ASV sequence
ASV_pu2_753_rfv	*Bifidobacterium*	TACGTAGGGCGCAAGCGTTATCCGGATTTATTGGGCGTAAAGGGCTCGT AGGCGGCTCGTCGCGTCCGGTGTGAAAGTCCATCGCTTAACGGTGGATC TGCGCCGGGTACGGGCGGGCTGGAGTGCGGTAGGGGAGACTGGAATTC CCGGTGTAACGGTGGAATGTGTAGATATCGGGAAGAACACCGATGGCG AAGGCAGGTCTCTGGGCCGTCACTGACGCTGAGGAGCGAAAGCGTGGG GAGCGAACAGG
ASV_8g8_d76_dba	*Staphylococcus*	TACGTAGGTGGCAAGCGTTATCCGGAATTATTGGGCGTAAAGCGCGCGT AGGCGGTTTTTTAAGTCTGATGTGAAAGCCCACGGCTCAACCGTGGAGG GTCATTGGAAACTGGAAAACTTGAGTGCAGAAGAGGAAAGTGGAATTC CATGTGTAGCGGTGAAATGCGCAGAGATATGGAGGAACACCAGTGGCG AAGGCGACTTTCTGGTCTGTAACTGACGCTGATGTGCGAAAGCGTGGGG ATCAAACAGG
ASV_1rx_gqy_wa1	*Enterococcus*	TACGTAGGTGGCAAGCGTTGTCCGGATTTATTGGGCGTAAAGCGAGCGC AGGCGGTTTCTTAAGTCTGATGTGAAAGCCCCCGGCTCAACCGGGGAGG GTCATTGGAAACTGGGAGACTTGAGTGCAGAAGAGGAGAGTGGAATTC CATGTGTAGCGGTGAAATGCGTAGATATATGGAGGAACACCAGTGGCG AAGGCGGCTCTCTGGTCTGTAACTGACGCTGAGGCTCGAAAGCGTGGG GAGCAAACAGG
ASV_qwa_h7y_hxz	*Streptococcus*	TACGTAGGTCCCGAGCGTTGTCCGGATTTATTGGGCGTAAAGCGAGCGC AGGCGGTTTGATAAGTCTGAAGTTAAAGGCTGTGGCTCAACCATAGTTC GCTTTGGAAACTGTCAAACTTGAGTGCAGAAGGGGAGAGTGGAATTCC ATGTGTAGCGGTGAAATGCGTAGATATATGGAGGAACACCGGTGGCGA AAGCGGCTCTCTGGTCTGTAACTGACGCTGAGGCTCGAAAGCGTGGGG AGCGAACAGG
ASV_9ec_9n4_k1l	*Escherichia-Shigella*	TACGGAGGGTGCAAGCGTTAATCGGAATTACTGGGCGTAAAGCGCACG CAGGCGGTTTGTTAAGTCAGATGTGAAATCCCCGGGCTCAACCTGGGAA CTGCATCTGATACTGGCAAGCTTGAGTCTCGTAGAGGGGGGTAGAATTC CAGGTGTAGCGGTGAAATGCGTAGAGATCTGGAGGAATACCGGTGGCG AAGGCGGCCCCCTGGACGAAGACTGACGCTCAGGTGCGAAAGCGTGGG GAGCAAACAGG
ASV_hg6_nng_f54	*Lactobacillus*	TACGTAGGTGGCAAGCGTTGTCCGGATTTATTGGGCGTAAAGCGAGCGC AGGCGGAAGAATAAGTCTGATGTGAAAGCCCTCGGCTTAACCGAGGAA CTGCATCGGAAACTGTTTTTCTTGAGTGCAGAAGAGGAGAGTGGAACTC CATGTGTAGCGGTGGAATGCGTAGATATATGGAAGAACACCAGTGGCG AAGGCGGCTCTCTGGTCTGCAACTGACGCTGAGGCTCGAAAGCATGGGT AGCGAACAGG
ASV_iwy_rb0_3yj	*Bifidobacterium*	TACGTAGGGTGCAAGCGTTATCCGGAATTATTGGGCGTAAAGGGCTCGT AGGCGGTTCGTCGCGTCCGGTGTGAAAGTCCATCGCTTAACGGTGGATC CGCGCCGGGTACGGGCGGGCTTGAGTGCGGTAGGGGAGACTGGAATTC CCGGTGTAACGGTGGAATGTGTAGATATCGGGAAGAACACCAATGGCG AAGGCAGGTCTCTGGGCCGTTACTGACGCTGAGGAGCGAAAGCGTGGG GAGCGAACAGG
ASV_c07_vnh_xuf	*Klebsiella*	TACGGAGGGTGCAAGCGTTAATCGGAATTACTGGGCGTAAAGCGCACG CAGGCGGTCTGTCAAGTCGGATGTGAAATCCCCGGGCTCAACCTGGGA ACTGCATTCGAAACTGGCAGGCTAGAGTCTTGTAGAGGGGGGTAGAAT TCCAGGTGTAGCGGTGAAATGCGTAGAGATCTGGAGGAATACCGGTGG CGAAGGCGGCCCCCTGGACAAAGACTGACGCTCAGGTGCGAAAGCGTG GGGAGCAAACAGG
ASV_71w_7js_dt9	*Streptococcus*	TACGTAGGTCCCGAGCGTTGTCCGGATTTATTGGGCGTAAAGCGAGCGC AGGCGGTTAGATAAGTCTGAAGTTAAAGGCTGTGGCTTAACCATAGTAC GCTTTGGAAACTGTTTAACTTGAGTGCAAGAGGGGAGAGTGGAATTCCA TGTGTAGCGGTGAAATGCGTAGATATATGGAGGAACACCGGTGGCGAA AGCGGCTCTCTGGCTTGTAACTGACGCTGAGGCTCGAAAGCGTGGGGA GCAAACAGG
ASV_85g_fdl_uzz	*Clostridium sensu stricto 1*	TACGTAGGTGGCGAGCGTTATCCGGATTTACTGGGCGTAAAGGGAGCGT AGGCGGATGATTAAGTGGGATGTGAAATACCCGGGCTCAACTTGGGTG CTGCATTCCAAACTGGTTATCTAGAGTGCAGGAGAGGAGAGTGGAATTC CTAGTGTAGCGGTGAAATGCGTAGAGATTAGGAAGAACACCAGTGGCG AAGGCGACTCTCTGGACTGTAACTGACGCTGAGGCTCGAAAGCGTGGG GAGCAAACAGG

Table S3. *Klebsiella pneumoniae* genome, Related to Figure 3.

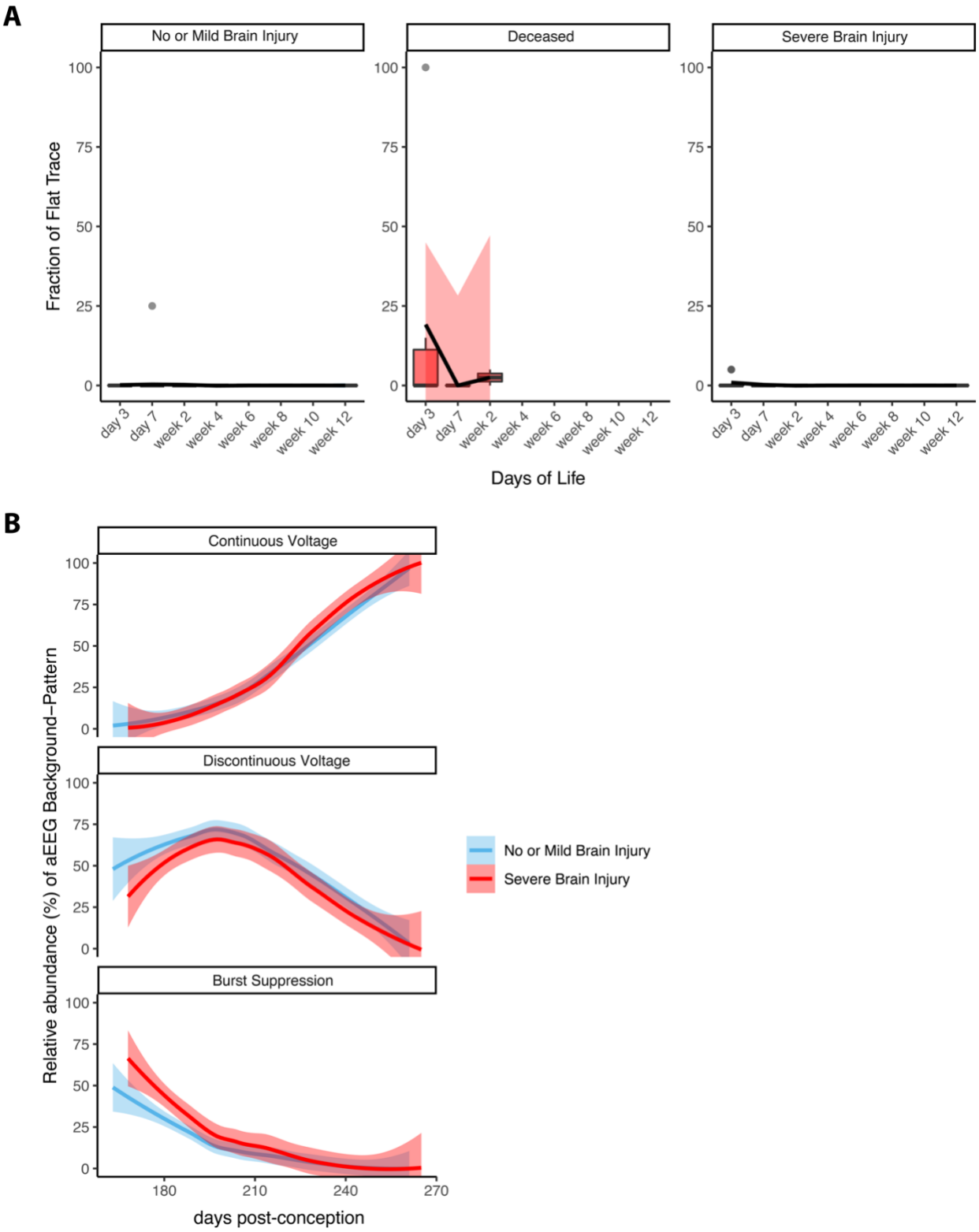

Figure S1. Neurophysiological development, Related to Figure 1. A) Flat Trace aEEG background pattern in infants with no or mild brain injury (BI), severe BI, and patients that died during hospitalization. B) aEEG background patterns i) Continuous Voltage (CV), ii)

Discontinuous Voltage (DV), iii) Burst Suppression (BS) over days post-conception. Infants without (blue) and with (red) severe BI. Boxplots show group median and interquartile range. Smoothed lines result from locally estimated scatterplot smoothing (LOESS) and indicate trends of neurophysiological development.

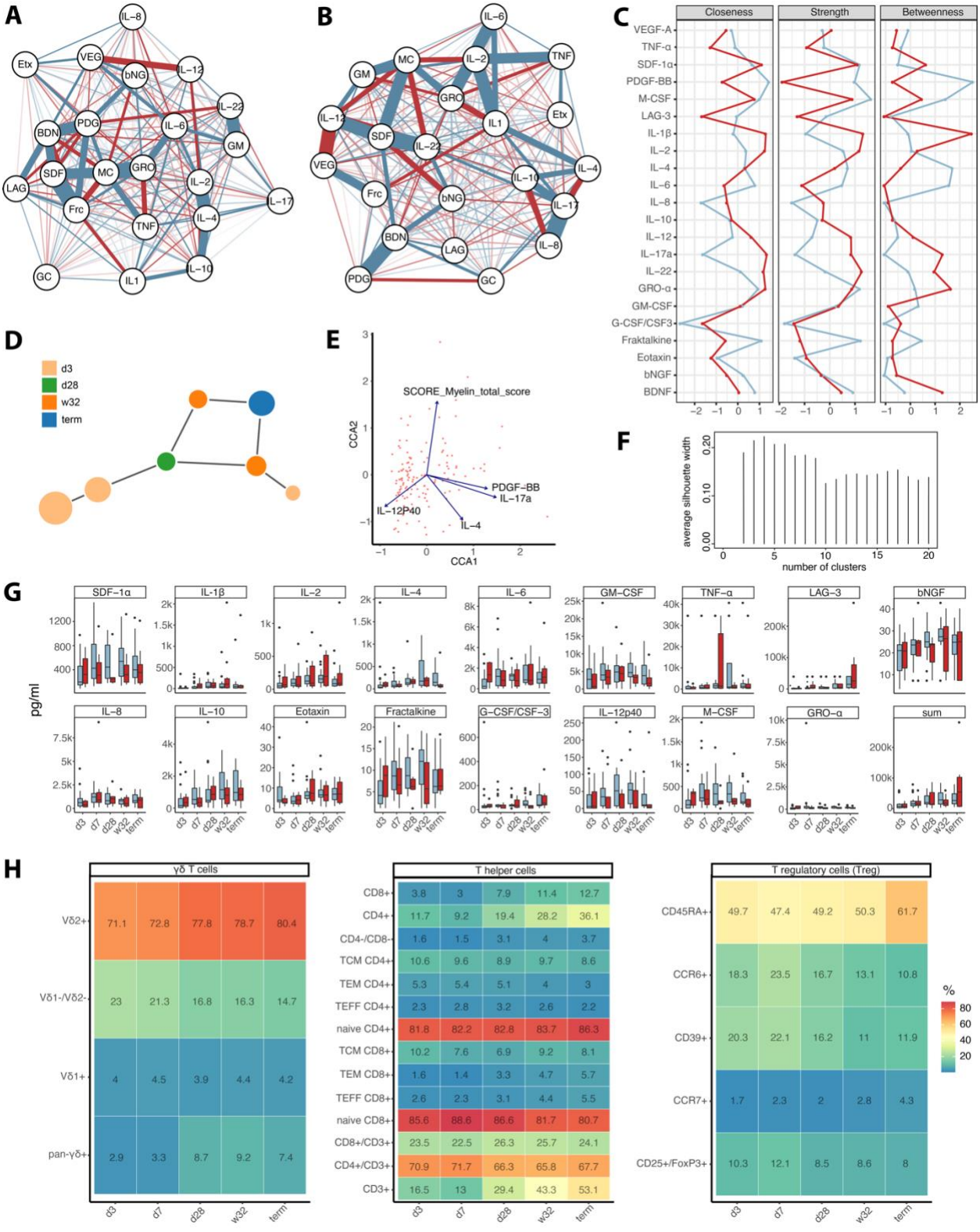

Figure S2. Immunological development, Related to Figure 2. A) Correlation network of stimulated cytokine values across all samples from infants without severe brain injuries (BI). B)

Correlation network of stimulated cytokine values across all samples from infants without severe BI. Positive Spearman correlations are blue and negative are red. The thickness of the connecting lines corresponds to the correlation strength. C) Connected dot-plots show closeness, strength, and betweenness of respective nodes between infants with (red) and without (blue) severe BI. D) Topographical data analysis of cytokine/chemokine levels. E) Canonical Correlation Analysis (CCA) of T cell profiles. Cytokines, chemokines, and neurodevelopmental scores that are significantly associated with the observed variation are shown as arrows. F) Silhouette clustering of blood cytokine and chemokine levels to determine the optimal number of Cyto-Clusters. G) Summary of all quantified cytokines and chemokines. Boxplots show group median and interquartile range. H) Summary of all quantified T cell receptors.

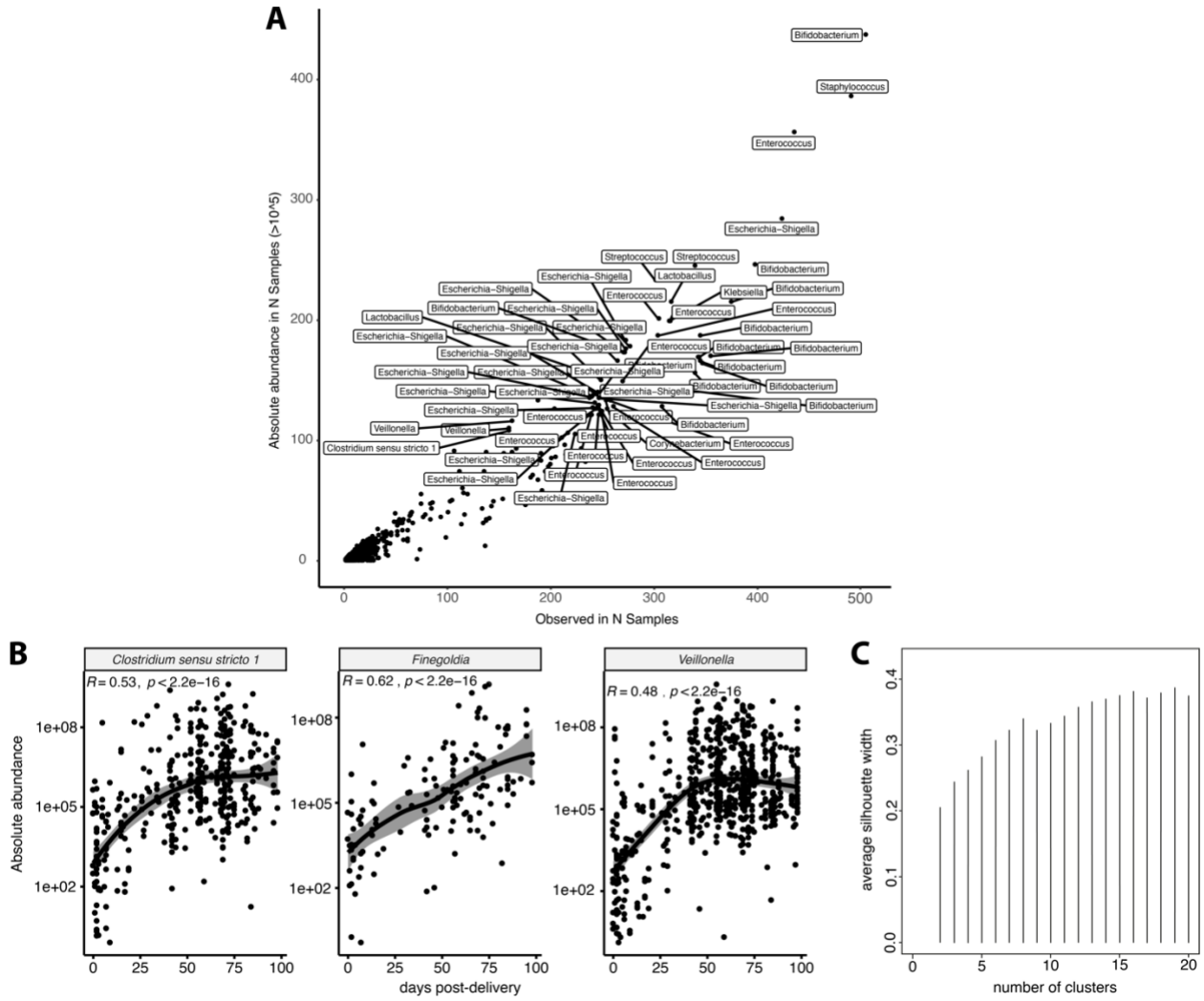

Figure S3. Microbiome development, Related to Figure 3. A) Core microbiome of extremely premature infants. Each dot represents a single observed ASV, positioned by its prevalence across all samples. Only ASVs that were observed in more than 20% of samples with an absolute abundance of $>10^5$ cells g^{-1} are labeled by their genus affiliation. B) Abundance of obligate anaerobic taxa with respect to days post-delivery. Smoothed lines result from locally estimated scatterplot smoothing (LOESS). Pearson correlation coefficient and p-value are shown. C) Silhouette clustering of absolute-abundance microbiome profiles to determine the optimal number of microbiome clusters.